

RESEARCH

Open Access



# The phytopathogen *Xanthomonas campestris* scavenges hydroxycinnamic acids *in planta* via the *hca* cluster to increase virulence on its host plant

Bo Chen<sup>1</sup>, Rui-Fang Li<sup>2</sup>, Lian Zhou<sup>3</sup>, Kai Song<sup>1</sup>, Alan R. Poplawsky<sup>4</sup> and Ya-Wen He<sup>1\*</sup> 

## Abstract

*Xanthomonas campestris* pv. *campestris* (*Xcc*) is the causal agent of black rot of cruciferous plants, which harbor high levels of hydroxycinnamic acids (HCAs) in their above-ground parts. Thus, upon infection of the host plant, the pathogen experiences a complex cocktail of HCAs. The present study shows that *Xcc* can efficiently degrade the HCAs, 4-hydroxycinnamic acid (4-HCA), ferulic acid (FA) and sinapic acid (SiA), via an *hca* cluster which encodes putative genes for a 4-hydroxycinnamoyl-CoA synthetase/4-HCA ligase HcaL, a benzaldehyde dehydrogenase HcaD, a 4-hydroxycinnamoyl-CoA hydratase/lyase HcaH and a member of the MarR-family of transcriptional factors, HcaR. *Xcc* also degrades the HCA caffeic acid, but with an alternative mechanism. RT-PCR and subsequent GUS assays show that the *hca* cluster is transcribed within a single operon, and its transcription is specifically induced by 4-HCA, FA and SiA. Furthermore, we show that HcaR negatively regulates *hca* transcription when its ligand, the proposed degradation pathway intermediate HCA-CoA, is not present. HcaR specifically binds to a 25-bp site, which encompasses the -10 elements of the *hca* promoter. Finally, GUS histochemical staining and subsequent quantitative analysis shows that the *hca* cluster is transcribed *in planta* during pathogenesis of Chinese radish, and *hca* deletion mutant strains exhibit compromised virulence in cabbage. Together, these results suggest that the ability to degrade HCAs contributes to *Xcc* virulence by facilitating its growth and spread, and by protecting the pathogen from HCA toxicity. A working model to explain *Xcc* HCA sensing and subsequent induction of the HCA degradation process is proposed.

**Keywords:** *Xanthomonas campestris*, 4-Hydroxycinnamic acid, *hca* cluster, Host-pathogen interaction, Pathogenicity

## Background

Plants produce diverse phenolic compounds, among which are the hydroxycinnamic acids (HCAs) such as 4-hydroxycinnamic acid (4-HCA), 2-hydroxycinnamic acid (2-HCA), ferulic acid (FA), sinapic acid (SiA) and caffeic acid (CA) (El-Seedi et al. 2012). In *Brassica*, HCAs

are abundant and often found conjugated to sugar moieties or other hydroxylic acids (Olsen et al. 2009; Lin and Harnly 2010; Cartea et al. 2010). In addition to their crucial roles in plant growth and development, HCAs also play important roles in plant defence. HCAs are broadly antimicrobial; they disrupt membrane integrity and decouple the respiratory proton gradient (Harris et al. 2010). HCAs also reinforce protective physical barriers in plants by cross-linking primary cell wall polysaccharides and by serving as precursors for lignin, which is a natural phenolic polymer that adds strength and rigidity to the plant cell wall (Naoumkina et al. 2010; Campos et al.

\*Correspondence: yawenhe@sjtu.edu.cn

<sup>1</sup> State Key Laboratory of Microbial Metabolism, Joint International Research Laboratory of Metabolic and Developmental Sciences, School of Life Sciences and Biotechnology, Shanghai Jiao Tong University, Shanghai 200240, China

Full list of author information is available at the end of the article



© The Author(s) 2022. **Open Access** This article is licensed under a Creative Commons Attribution 4.0 International License, which permits use, sharing, adaptation, distribution and reproduction in any medium or format, as long as you give appropriate credit to the original author(s) and the source, provide a link to the Creative Commons licence, and indicate if changes were made. The images or other third party material in this article are included in the article's Creative Commons licence, unless indicated otherwise in a credit line to the material. If material is not included in the article's Creative Commons licence and your intended use is not permitted by statutory regulation or exceeds the permitted use, you will need to obtain permission directly from the copyright holder. To view a copy of this licence, visit <http://creativecommons.org/licenses/by/4.0/>.

2014; Liu et al. 2018). Due to their antioxidant and antimicrobial activities, the increased accumulation of phenolic acids can aid in plant defence against pathogens. For example, grapevines infected with *Xylella fastidiosa* accumulated FA in their xylem cell walls (Wallis and Chen 2012), and 4-HCA and FA were induced in barley root exudates after *Fusarium* inoculation (Lanoue et al. 2010). In addition, non-lethal concentrations of 4-HCA and 2-HCA have been shown to interfere with the type III secretion system (T3SS) of *Dickeya dadantii*, and pretreatment of *Xanthomonas oryzae* with 2-HCA reduced the disease symptoms observed on rice via a T3SS-specific inhibition (Yang et al. 2008; Li et al. 2009; Fan et al. 2017).

A multitude of bacterial species participate in the decomposition of plant residues and make a major contribution to the recycling of aromatic compounds (Fuchs et al. 2011). The catabolism of HCAs has been reported in several environmental or rhizosphere bacterial species such as *Rhodopseudomonas palustris* CGA009, *Sphingobium* sp. SYK-6, *Agrobacterium fabrum*, *Pseudomonas*, *Acinetobacter* sp. ADP1, *Ralstonia solanacearum* and *Rhodococcus jostii* RHA1 (Parke and Ornston 2003; Lowe et al. 2015; Hirakawa et al. 2012; Campillo et al. 2014; Calero et al. 2018; Meyer et al. 2018). The two major pathways for the degradation of 4-HCA into 4-hydroxybenzoic acid (4-HBA) are the CoA-dependent  $\beta$ -oxidation and the CoA-dependent non- $\beta$ -oxidation pathways (Parke and Ornston 2003; Campillo et al. 2014; Calero et al. 2018). Both pathways are initiated by CoA activation of the 4-HCA carboxylate side chain to generate a hydroxycinnamoyl-CoA. In *Rhodopseudomonas palustris*, *Acinetobacter* sp. ADP1 and *Ralstonia solanacearum*, the catabolism of 4-HCA, FA and CA follows the CoA-dependent non- $\beta$ -oxidation pathway (Parke and Ornston 2003; Hirakawa et al. 2012; Kasai et al. 2012).

*X. campestris* pv. *campestris* (*Xcc*) is an obligate aerobic, gram-negative bacterium that causes black rot, a devastating, systemic, vascular disease of *Brassica* species (Vicente and Holub 2013). Due to its agricultural importance, numerous studies on its diverse virulence factors have established *Xcc* as a model organism for the study of plant-pathogen interactions (Mansfield et al. 2012; Timilsina et al. 2020). As a vascular phytopathogen, *Xcc* is exposed to diverse phenolic compounds during infection of its host plant. In addition to the endogenously biosynthesized phenolic acids, multiple degradative enzymes produced by *Xcc* cleave the plant cell wall to generate simple sugars and also release lignin, which, when hydrolyzed forms various types of phenolic acids such as HCAs, vanillic acid and 4-HBA (Bertani et al. 2001). Our previous findings revealed that *Xcc* can sense 4-HBA and convert 4-HBA into protocatechuate (PCA)

via the *pobA/pobR* locus (Chen et al. 2020). PCA can be further converted into succinyl-CoA and acetyl-CoA via the  $\beta$ -ketoacid pathway (Wang et al. 2015). Disruption of the pathogen's 4-HBA or PCA degradation pathways results in significantly reduced virulence (Wang et al. 2015; Chen et al. 2020), suggesting that successful *Xcc* infection may be partially dependent on the catabolism of plant-derived phenolic compounds. How *Xcc* overcomes cell wall lignification and HCAs to cause disease is not yet fully understood.

In this current study we initially analyze the role of an *hca* gene cluster in 4-HCA, FA and CA catabolism, and characterize the expression patterns of this gene cluster in *Xcc* strain XC1. The molecular mechanisms underlying the inductive transcription of this gene cluster are further investigated, and finally we show that this gene cluster is transcribed during *Xcc* infection of Chinese radish and is required for full pathogenicity of *Xcc*.

## Results

### Cabbage leaf tissues contain pico-molar levels of HCAs

To quantitatively determine the relative level of HCAs in cabbage leaf tissues, micro levels of commercially available 4-HCA, FA, SiA, CA, 2-HCA and 3-HCA in aqueous solution were assayed using Ultra-High Performance Liquid Chromatography coupled with Triple Quadrupole Tandem Mass Spectrometry (UHPLC-TQT-MS). Quantitative standard curves were established for each of the HCAs (Fig. 1a and Additional file 1: Fig. S1). Endogenous HCAs were then extracted from the leaves of 2-month-old cabbage plants using the previously described methods of Pan et al. (2010). UHPLC-TQT-MS analysis identified 4-HCA, FA, SiA and CA from these cabbage leaf tissues at levels ranging from 55.6 to 173.2 pmol/g fresh weight (Fig. 1b). We could detect neither 2-HCA nor 3-HCA in cabbage leaf tissues.

### *Xcc* degrades 4-HCA into 4-HBA via the *hca* gene cluster

To determine whether *Xcc* can degrade HCAs, 4-HCA, FA, SiA, CA, 2-HCA and 3-HCA were independently added to separate NYG cultures of wild-type strain XC1 at a final concentration of 50  $\mu$ M. The cultures were then collected every 12 h for quantitative assay of HCA levels. The levels of 4-HCA, FA, SiA and CA decreased over time during XC1 growth in NYG medium (Fig. 1c), whereas the levels of HCAs incubated in NYG medium without the addition of XC1 did not change significantly (Additional file 1: Fig. S2a). FA was degraded most efficiently by XC1, followed by 4-HCA, SiA and CA. 2-HCA and 3-HCA were not degraded by XC1 (Fig. 1c).

Previously, the gene cluster PP\_3356–PP\_3359 was experimentally shown to be responsible for 4-HCA degradation in *Pseudomonas putida* strain KT2440

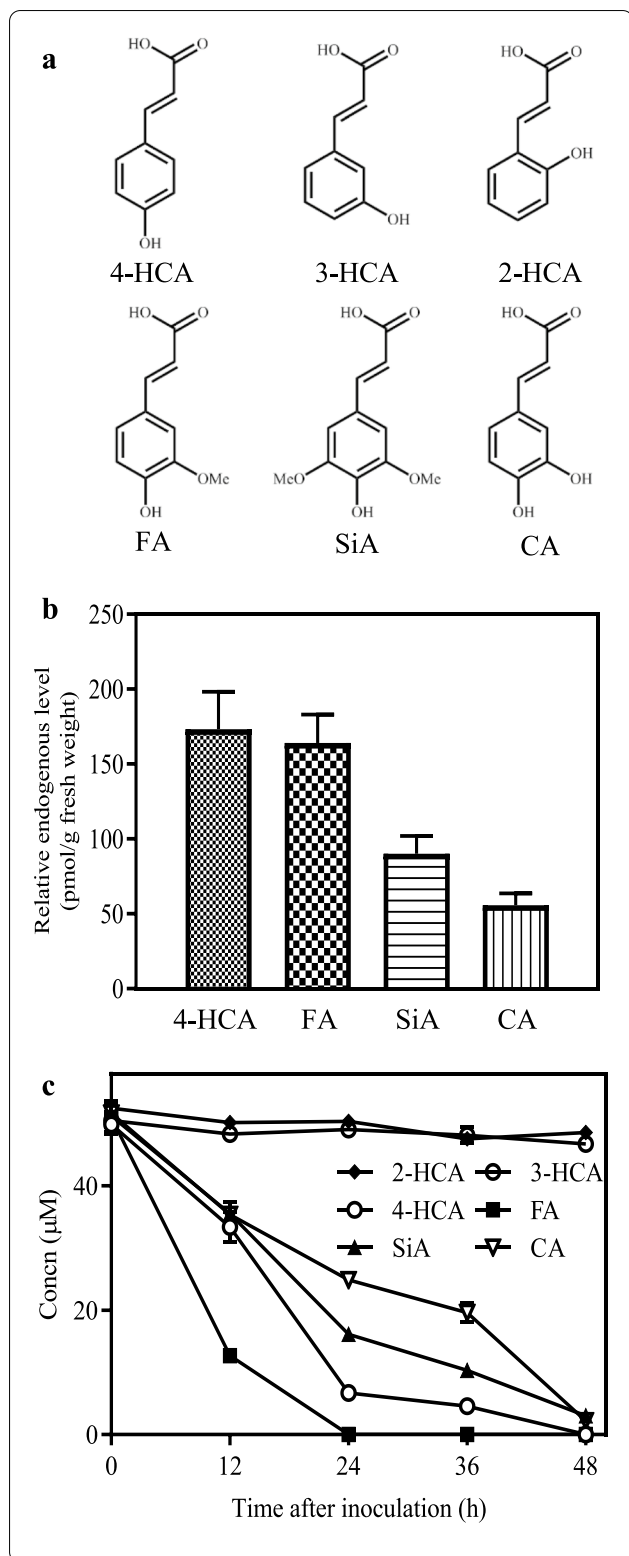


**Fig. 1** Hydroxycinnamic acid degradation by strain XC1 of *Xcc*.

**a** The chemical structures of hydroxycinnamic acids. 2-HCA, 2-hydroxycinnamic acid; 3-HCA, 3-hydroxycinnamic acid; 4-HCA, 4-hydroxycinnamic acid; FA, ferulic acid; SiA, sinapic acid; CA, caffeic acid. **b** The relative endogenous levels of 4-HCA, FA, SiA and CA in leaf tissues of cabbage. **c** Time course of hydroxycinnamic acid degradation in NYG cultures of strain XC1. Three independent experiments were conducted and values are shown as averages with standard deviations

XCCB100\_3542–XCCB100\_3545 (*hca* in this study) which encodes putative genes for 4-hydroxycinnamoyl-CoA synthetase/4-HCA ligase (*HcaL*), benzaldehyde dehydrogenase (*HcaD*, 490 aa), 4-hydroxycinnamoyl-CoA hydratase/lyase (*HcaH*) and a multiple antibiotic resistance regulator (*MarR*)-family transcriptional regulator (*HcaR*) (Fig. 2a). Although sequence analysis indicated that *Xcc* strains XC1, CN14 and CN16 contained this same *hca* gene cluster (Additional file 1: Fig. S3a; <https://www.ncbi.nlm.nih.gov/genome/>), the *hca* cluster in *Xcc* strains ATCC33913 and 8004 was comprised of 5 genes (Additional file 1: Fig. S3a). In these strains the loss of a G residue in the *hcaD* DNA sequence caused a frameshift which resulted in a stop codon and a truncated 384 aa *HcaD* (Additional file 1: Fig. S3b). Consequently, a new gene (*Xcc0808* in ATCC33913 or *XC\_3422* in 8004) was annotated in these two strains downstream of *hcaD* (Additional file 1: Fig. S3b).

To examine the possible involvement of the *Xcc hca* gene cluster in 4-HCA catabolism, a series of mutant strains,  $\Delta hcaL$ ,  $\Delta hcaD$  and  $\Delta hcaH$ , were generated in the wild-type strain XC1. When grown in NYG medium supplemented with 50  $\mu$ M 4-HCA, all the mutant strains displayed similar growth to the wild-type strain XC1 (Fig. 2b). The 4-HCA levels in the XC1 culture declined over time while the 4-HCA levels in the cultures of  $\Delta hcaL$  and  $\Delta hcaH$  remained relatively constant during growth (Fig. 2c). Overexpression of *hcaL* or *hcaH* via the vector pBBRMCS in  $\Delta hcaL$  or  $\Delta hcaH$  restored their 4-HCA degradation abilities to the level of wild-type XC1 (Fig. 2c). These results suggest that *hcaL* and *hcaH* are essential for 4-HCA degradation in XC1. In contrast, 4-HCA levels in the  $\Delta hcaD$  culture declined over time, although they remained significantly higher than those in the XC1 culture at all growth points (Fig. 2c). Overexpression of *hcaD* in the mutant strain  $\Delta hcaD$  restored the 4-HCA degradation ability to that of the wild-type strain XC1 (Fig. 2c). These results suggest that although *HcaD* is also involved in 4-HCA degradation, a *HcaD* homolog may be present in XC1.

Our previous results showed that *Xcc* can produce 4-HBA via *xanB2* and degrade 4-HBA via *pobA* and the

(Plaggenborg et al. 2003). Using this gene cluster as a template and the *Xcc* strain B100 DNA sequence, Blast analysis identified the homologous gene cluster

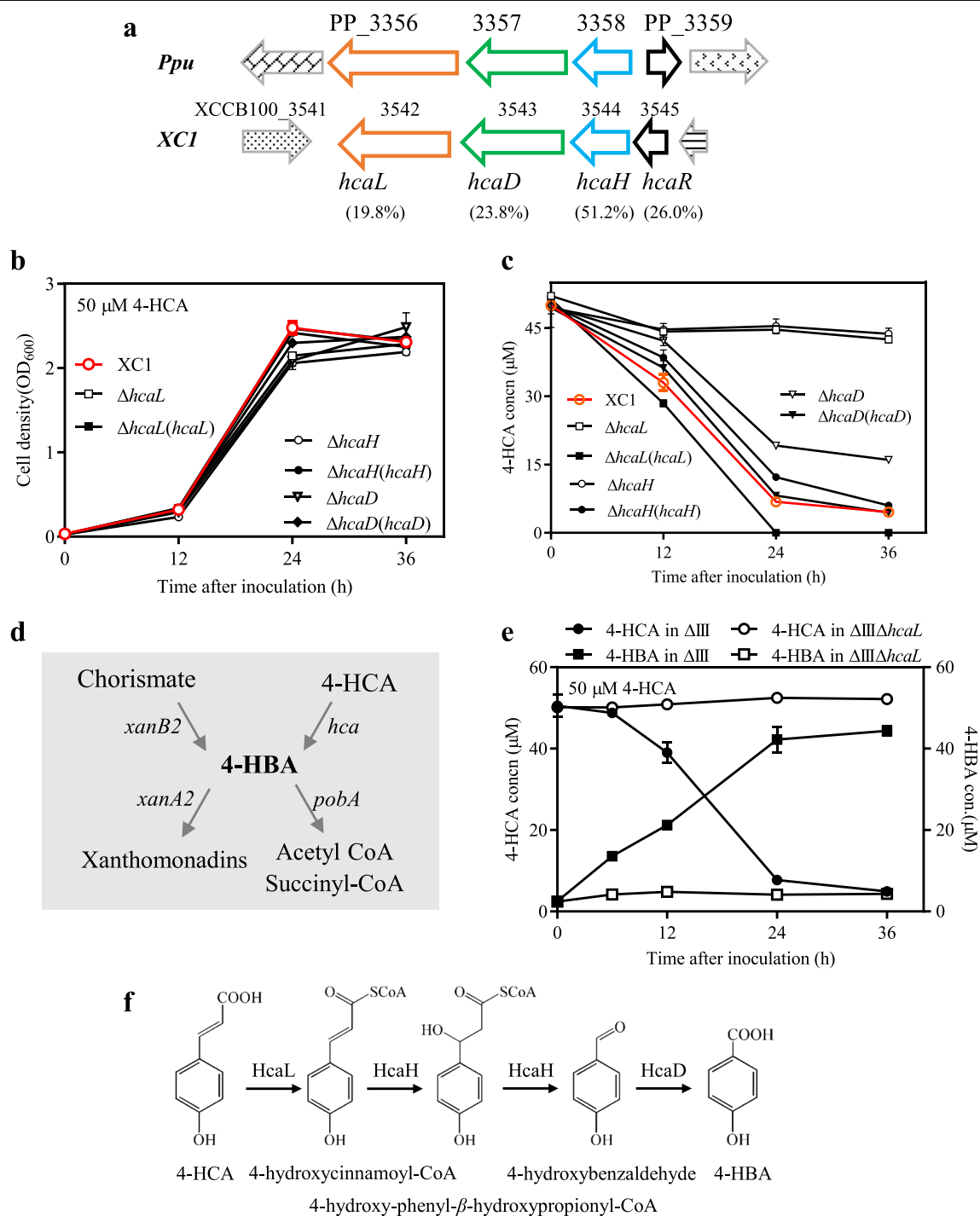


**Fig. 2** 4-HCA degradation in strain XcI of *Xcc* via the *hca* gene cluster. **a** Using the gene cluster PP\_3356–PP\_3359 which is involved in 4-HCA degradation in *Pseudomonas putida*, homology analysis identified a putative 4-HCA degradation gene cluster, *hca* in *Xcc* (colored arrows). *hcaL* encodes a putative 4-hydroxycinnamoyl-CoA ligase; *hcaD* encodes a benzaldehyde dehydrogenase; *hcaH* encodes a 4-hydroxycinnamoyl-CoA hydratase/lyase, and *hcaR* encodes a MarR-family transcriptional regulator. The numbers inside the parentheses indicate the amino acid identity. **b** Growth time course of XcI and XcI-derived mutants in NYG medium supplemented with 50  $\mu$ M 4-HCA. **c** Time course for 4-HCA production by strain XcI, XcI-derived mutants and restored mutants in NYG cultures supplemented with 50  $\mu$ M 4-HCA. **d** A simple schematic diagram of 4-HBA synthesis, utilization and degradation processes in *Xcc*. **e** Time course of 4-HCA and 4-HBA production of strains  $\Delta xanB2\Delta xanA2\Delta poba$  ( $\Delta III$ ) and  $\Delta xanB2\Delta xanA2\Delta poba\Delta hcaL$  ( $\Delta III\Delta hcaL$ ). **f** The proposed 4-HCA degradation pathway in *Xcc*. For the data in (b, c and e), three independent experiments were conducted for each and the averages with standard deviations are shown

subsequent *pca* cluster in XC1 (Zhou et al. 2013; Wang et al. 2015; Chen et al. 2020). Further study showed that *Xcc* can use 4-HBA to synthesize the yellow pigment xanthomonadin via *xanA2* (Cao et al. 2020) (Fig. 2d). In this study, a triple deletion mutant  $\Delta xanB2\Delta pobA\Delta xanA2$  ( $\Delta III$  in this study) was generated. This triple mutant strain cannot produce 4-HBA and also cannot degrade 4-HBA; thus, it can be used to test whether 4-HBA is the end product of 4-HCA degradation via the *hca* gene cluster. When mutant strain  $\Delta III$  was grown in NYG medium supplemented with 50  $\mu$ M 4-HCA, 4-HCA levels decreased over time while 4-HBA levels in the same culture increased over the same time period (Fig. 2e). Furthermore, when *hcaL* was deleted in strain  $\Delta III$  to generate strain  $\Delta III\Delta hcaL$ , which was then grown in NYG medium supplemented with 50  $\mu$ M 4-HCA, 4-HCA levels remained constant, and significant levels of 4-HBA were not detected (Fig. 2e). Taken together, these results strongly suggest that the end product of 4-HCA degradation via the *hca* cluster is 4-HBA (Fig. 2f).

#### ***Xcc* also degrades FA and SiA, but not CA, via the *hca* gene cluster**

Parent strain XC1, and mutant strains  $\Delta hcaL$ ,  $\Delta hcaL(hcaL)$ ,  $\Delta hcaD$ ,  $\Delta hcaD(hcaD)$ ,  $\Delta hcaH$  and  $\Delta hcaH(hcaH)$  were individually grown in NYG medium supplemented with either 50  $\mu$ M FA, 50  $\mu$ M SiA or 50  $\mu$ M CA, and the levels of these HCAs were examined during growth. Deletion of *hcaL* or *hcaH* abolished *Xcc*'s ability to degrade FA and SiA while deletion of *hcaD* significantly reduced the ability of *Xcc* to degrade FA and SiA (Additional file 1: Fig. S4a–d). Overexpression of either *hcaL*, *hcaD* or *hcaH* restored the mutants' abilities to degrade FA and SiA (Additional file 1: Fig. S4a–d). In contrast, the deletion of *hcaL*, *hcaD* or *hcaH* had little effect on the ability of *Xcc* to degrade CA (Additional file 1: Fig. S2). These results suggest that *Xcc* uses the *hca* gene cluster to degrade FA and SiA but probably uses an alternative pathway to degrade CA. Based on previous findings and this current genetic study, the degradation pathways of FA and SiA in *Xcc* were proposed as shown in Additional file 1: Fig. S4e.

#### **HcaR negatively regulates *hcaR* expression as well as the degradation of 4-HCA, FA and SiA**

*hcaR* encodes a putative 156-amino acid transcriptional factor with a MarR-family helix-turn-helix (HTH) DNA

binding domain (Fig. 3a). To test its effect on HCA degradation, *hcaR* was deleted in XC1. The resultant strain  $\Delta hcaR$  displayed a growth pattern similar to that of the wild-type strain XC1 in NYG medium supplemented with 50  $\mu$ M 4-HCA (Fig. 3b). However, the 4-HCA degradation activity of strain  $\Delta hcaR$  was significantly higher than that of the wild-type strain XC1 (Fig. 3c). Overexpression of *hcaR* via the expression vector pBBR-1-MCS in strain  $\Delta hcaR$  significantly restored 4-HCA degradation activity to a level higher than that of the wild-type strain XC1 (Fig. 3c). Although not as dramatic, the effects of *hcaR* on FA and SiA degradation were similar to those observed with 4-HCA (Fig. 3d, e). These results suggest that HcaR negatively regulates the degradation of 4-HCA, FA and SiA in *Xcc*.

Subsequently, two reporter strains, XC1::P<sub>hca</sub>-*gusA* and  $\Delta hcaR$ ::P<sub>hca</sub>-*gusA*, were generated to verify the negative regulation of *hca* expression by HcaR. In the absence of HCAs, *hca* expression was not observed in XC1::P<sub>hca</sub>-*gusA*, however a high level of expression was observed in  $\Delta hcaR$ ::P<sub>hca</sub>-*gusA* (Fig. 3f). These results suggest that HcaR negatively regulates *hcaR* expression and subsequently the degradation of 4-HCA, FA and SiA in *Xcc*.

#### **Transcription of the *hca* gene cluster is negatively regulated by HcaR and specifically induced by 4-HCA, FA and SiA**

In the *P. putida* 4-HCA degradation gene cluster, the gene encoding HcaR (PP\_3359) is divergently transcribed from the genes encoding HcaL, HcaH and HcaD (PP\_3356–PP\_3358) (Fig. 2a). However, *hcaR* is transcribed in the same orientation as the other *hca* genes in *Xcc* strains (Fig. 2a and Additional file 1: Fig. S3), possibly all from the same promoter. We initially used PCR and reverse transcription-PCR (RT-PCR) analysis to test whether the *Xcc hca* is transcribed as a single operon. PCR analysis of XC1 genomic DNA confirmed that specific primers designed to amplify *hca* intergenic regions were functional (Fig. 4a, lanes 1). Then, using RT-PCR of XC1 total RNA harvested at 24 hpi (hours post-inoculation) in NYG medium supplemented with 50  $\mu$ M 4-HCA, we identified the same three specific PCR products that correspond to the three intergenic regions of the *hca* cluster (Fig. 4a, lanes 3). Finally, simple PCR reactions with these same RNA preparations gave negative results,

(See figure on next page.)

**Fig. 3** The effect of HcaR on HCA degradation. **a** The domain organization of HcaR in *Xcc*. **b** Growth time course of XC1,  $\Delta hcaR$  and  $\Delta hcaR(hcaR)$  in NYG medium supplemented with 50  $\mu$ M 4-HCA. **c–e** Time course of HCA production by XC1,  $\Delta hcaR$  and  $\Delta hcaR(hcaR)$  in NYG liquid medium supplemented with 50  $\mu$ M 4-HCA, 50  $\mu$ M 4-FA or 50  $\mu$ M CA. **f** Relative GUS activities of two reporter strains, XC1::P<sub>hca</sub>-*gusA* and  $\Delta hcaR$ ::P<sub>hca</sub>-*gusA* when grown on NYG agar or liquid medium in the absence of HCAs. Averages with standard deviations of three independent experiments are shown

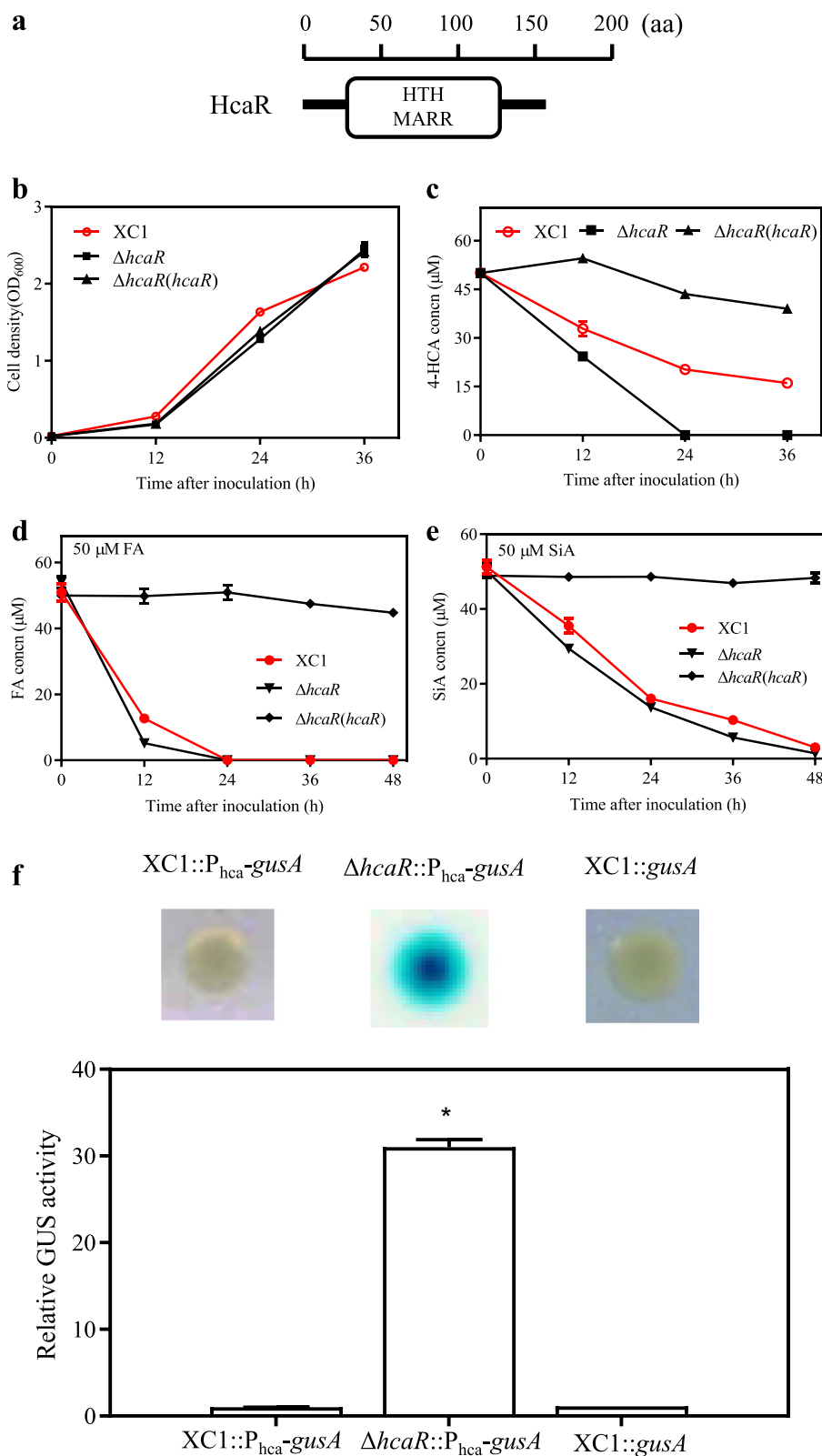


**Fig. 3** (See legend on previous page.)

confirming the absence of DNA contamination (Fig. 4a, lanes 2). These results showing that the *hca* intergenic region sequences are found on mRNA suggested that *hcaR* and the other *hca* genes are all part of the same transcript. To further confirm these findings, each of the upstream DNA fragments (~500 bp) of *hcaR*, *hcaH*, *hcaD* and *hcaL*, ( $P_{hca}$ ,  $P_{hcaH}$ ,  $P_{hcaD}$ ,  $P_{hcaL}$ , respectively), was cloned, individually fused with *gusA*, and used to generate the strains  $XC1::P_{hca}-gusA$ ,  $XC1::P_{hcaH}-gusA$ ,  $XC1::P_{hcaD}-gusA$  and  $XC1::P_{hcaL}-gusA$  (Additional file 1: Fig. S5a, b). These strains were then used for promoter activity assays. When tested on either NYG agar or in NYG liquid medium supplemented with 50 mg/L X-gluc and 50  $\mu$ M 4-HCA, only strain  $XC1::P_{hca}-gusA$  displayed GUS activity (Fig. 4b). These results confirmed that only  $P_{hca}$  has promoter activity and that *hcaR* is co-transcribed with the other *hca* genes as a single operon.

Using the constructed reporter strain  $XC1::P_{hca}-gusA$ , *hca* transcription was also monitored in the presence of other hydroxycinnamic acids. On NYG agar medium supplemented with 4-HCA, FA or SiA (50  $\mu$ M and 200  $\mu$ M), colonies were blue, indicating that *hca* expression was induced (Fig. 4c). In contrast, using agar plates supplemented with CA, 4-HBD or vanillin, no GUS-dependent blue color was observed in the reporter strain  $XC1::P_{hca}-gusA$  (Fig. 4c). During growth in liquid NYG culture, the  $P_{hca}$ -dependent GUS activities increased up to 50-fold as the concentrations of 4-HCA, FA or SiA increased from 50 to 200  $\mu$ M (Fig. 4c). However, the addition of CA, 4-HBD or vanillin had little effect on the GUS activities of  $XC1::P_{hca}-lacZ$  (Fig. 4c). These results suggest that *hca* transcription is specifically induced by 4-HCA, FA and SiA.

#### 4-HCA-CoA, FA-CoA and SiA-CoA are ligands of HcaR

The ligand-free form of MarR-family transcriptional factors binds to cognate nucleotide operator sequences to repress transcription, and this binding is antagonized in the presence of a ligand. For example, in the 4-HCA-degrading soil bacterium *Rhodococcus jostii* RHA1, the HcaR homolog CouR first forms a dimer and then binds two molecules of the catabolite 4-HCA-CoA. Thus, the presence of 4-HCA-CoA prevents the binding of CouR to

its operator DNA in vitro (Otani et al. 2016). Based on the degradation pathways of 4-HCA, FA and SiA (Fig. 2f and Additional file 1: Fig. S4e), in the presence of 50  $\mu$ M HCAs, HCA-CoAs should be accumulated in strain  $\Delta hcaH$ , but not in strain  $\Delta hcaL$ . To study the ligand of HcaR in *Xcc*, two reporter strains  $\Delta hcaL::P_{hca}-gusA$  and  $\Delta hcaH::P_{hca}-gusA$  were generated in this study. On NYG agar plates supplemented with 50  $\mu$ M 4-HCA, FA or SiA, the two reporter strains grew well and  $P_{hca}$ -dependent GUS activity was observed in strain  $\Delta hcaH::P_{hca}-gusA$  but not in strain  $\Delta hcaL::P_{hca}-gusA$  (Fig. 5a). Similar results were observed when these strains were grown in liquid NYG medium supplemented with 50  $\mu$ M HCAs (Fig. 5b). These results demonstrate that the HcaL-catalyzed reaction products, 4-hydroxycinnamoyl-CoA, feruloyl CoA and sinapoyl CoA are ligands of HcaR.

#### HcaR specifically binds to a 25-bp site in the *hca* promoter region

Heterologous expression of the full-length *Xcc hcaR* gene in *E. coli* via the expression vector pET-28a yielded soluble protein (Fig. 6a), and purified HcaR formed a dimer in solution (Additional file 1: Fig. S6). Electrophoretic mobility shift assays (EMSA) were then conducted to examine the DNA-binding activity of HcaR to a 183-bp DNA fragment encompassing the *hca* promoter region,  $P_{hca}$  (10 nM). As shown in Fig. 6b, a significant shift of labeled DNA was observed in the presence of increasing concentrations (0.05–5.0 nM) of HcaR. In the presence of high levels of unlabeled probes (2000 nM), no more shift was observed (Fig. 6b, lane 8). These results indicate a specific binding between HcaR and  $P_{hca}$ .

To identify the precise HcaR binding site, a DNase I foot-printing analysis was performed. A representative sequencing result is shown in Fig. 6c. The data show that HcaR can protect a 25-bp DNA region “CTAGATTGT ATTTCATGGATAACAAT” from DNase I digestion. The HcaR binding site fully overlapped the -10 box in the *hca* promoter (Fig. 6d). Additionally, an alignment of the *hca* promoter sequences from 9 *Xanthomonas* genomes revealed a putative inverted repeat sequence ATTGTA T-ATACAAT (Additional file 1: Fig. S7). Such inverted repeats are characteristic of the nucleotide sequences

(See figure on next page.)

**Fig. 4** Transcription of the *hca* gene cluster. **a** RT-PCR analysis of the *hca* gene cluster. Lanes 1–4 indicate agarose gel analysis of PCR products generated with the indicated primers and using the following templates: XC1 genomic DNA(1); total RNAs from 4-HCA-treated XC1(2); cDNA from total RNAs of 4-HCA-treated XC1(3); ddH<sub>2</sub>O(4). **b** Colonies of four promoter-driven strains on NYG agar media supplemented with 50  $\mu$ g/mL x-Gluc in the absence or presence of 50  $\mu$ M 4-HCA and GUS activities of four promoter-driven strains in NYG liquid medium in the presence of 50  $\mu$ M 4-HCA. **c** Colonies of strain  $XC1::P_{hca}-gusA$  grown on NYG agar medium supplemented with 50  $\mu$ g/mL of x-Gluc and different HCAs and GUS activities of strain  $XC1::P_{hca}-gusA$  grown on NYG medium with various HCAs added (0–200  $\mu$ M). Three independent experiments were conducted and average values with standard deviations are shown. Values in treatments with HCAs added which were significantly different from the value in the absence of HCAs are indicated by one ( $P < 0.05$ ), two ( $P < 0.01$ ) or three ( $P < 0.001$ ) asterisks

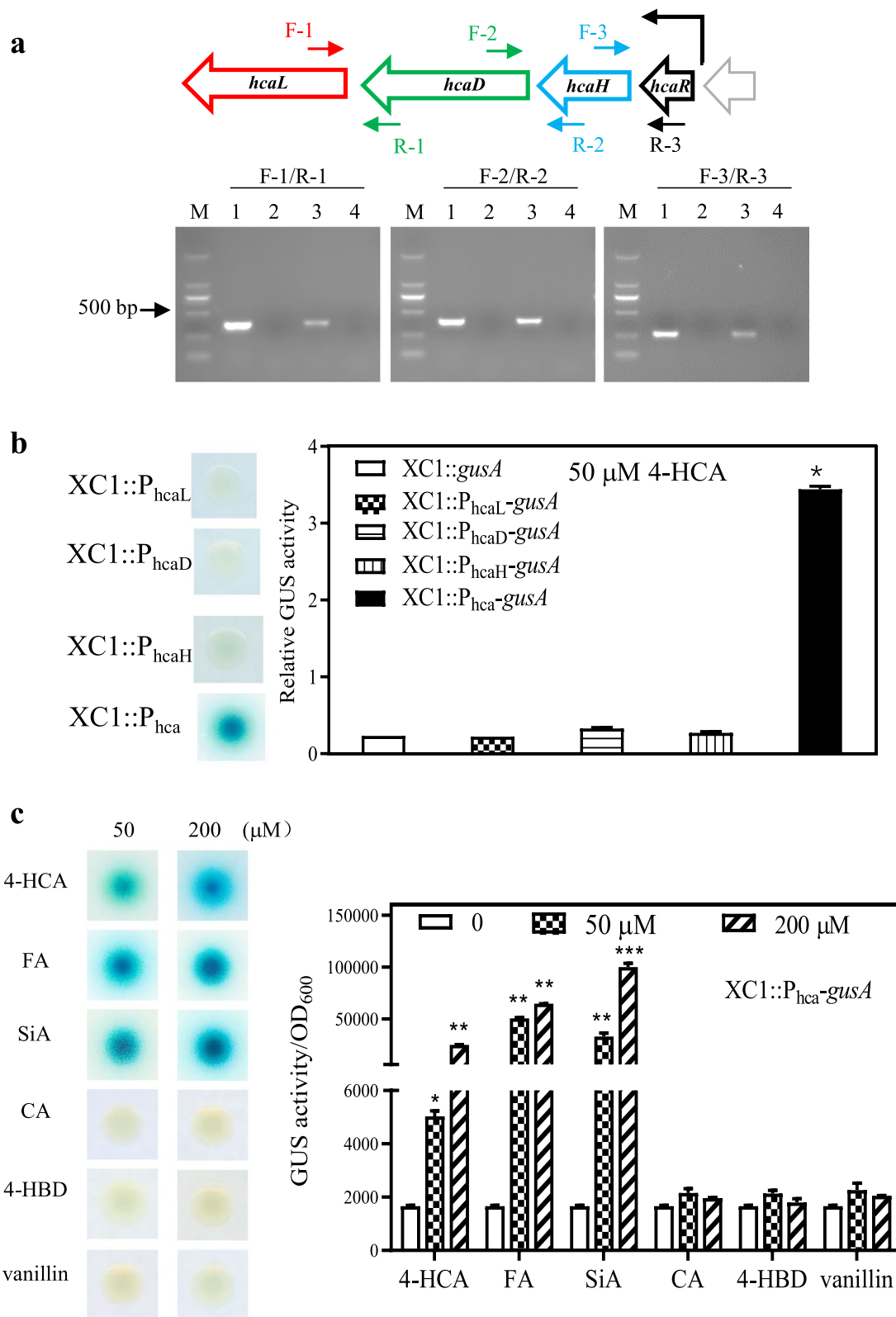
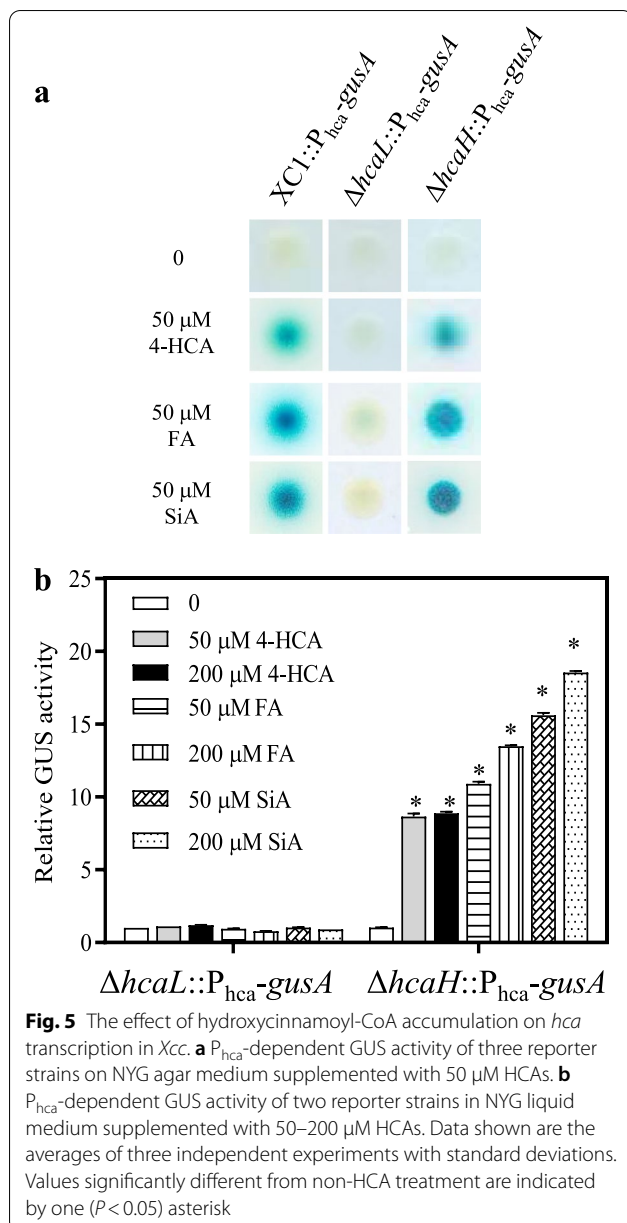


**Fig. 4** (See legend on previous page.)



recognized by MarR family transcriptional regulators (Otani et al. 2016). When the ATGTAT sequence was converted to CCCCCC and the resultant variant was subjected to EMSA analysis for HcaR binding ability, this

variant was unable to bind to HcaR (Fig. 6e). This result verifies the key role of the inverted repeat sequence in HcaR binding.

#### The *hca* cluster is transcribed during XC1 infection of Chinese radish

*Xcc* is a xylem-dwelling phytopathogen and the conditions for *Xcc in planta* growth are probably different from those required for growth in culture. To elucidate the role of the *hca* cluster in *Xcc* pathogenesis, it must be determined whether the *hca* cluster is expressed during disease development. To this end, the XC1 strain carrying the *hca* reporter gene construct  $XC1::P_{hca}-gusA$  was introduced into Chinese radish.  $XC1::gusA$  carrying a promoterless *gusA* gene and the previously constructed *pobA* reporter strain  $XC1::P_{pobA}-gusA$  (Chen et al. 2020) were used as negative and positive control strains, respectively.

Histochemical staining analysis detected  $P_{hca}$ -dependent GUS expression in the infected leaf tissues (Fig. 7a). No significant differences in bacterial population levels (CFUs) were observed between the reporter strains in any of the infected leaves analyzed at 3 and 5 days post-inoculation (dpi) (Fig. 7a). Subsequent GUS quantitative assays demonstrated that the expression level of the *hca* cluster was comparable to that of *pobA* inside the infected tissues (Fig. 7b).

#### The *hca* cluster is required for full virulence of XC1 in cabbage

We further characterized the virulence levels of *hca* mutants,  $\Delta hcaL$ ,  $\Delta hcaD$ ,  $\Delta hcaH$  and  $\Delta hcaR$ , in cabbage (Jingfeng-1) using the leaf-clipping method (Fig. 7c). At 15 dpi, the average lesion lengths of strains  $\Delta hcaL$ ,  $\Delta hcaD$ ,  $\Delta hcaH$  and  $\Delta hcaR$  in cabbage were 8.3 mm, 10.2 mm, 3.9 mm and 11.2 mm, respectively (Fig. 7d); all significantly shorter than that of the wild-type strain XC1 (15.9 mm).

#### The *hca* cluster is conserved in the phytopathogens *Xanthomonas*

A BLAST analysis of the NCBI Nr database revealed that the *hca* cluster is present in the genomes of almost all *Xanthomonas* species, including: *Xcc*, *X. citri* pv. *citri*, *X. campestris* pv. *raphanin*, *X. campestris* pv. *vesicatoria*,

(See figure on next page.)

**Fig. 6** Electrophoretic mobility shift assays (EMSA) for the identification of the HcaR binding site in the promoter region of the *hca* operon. **a** SDS-PAGE analysis of the purified HcaR protein. **b** EMSA was performed using a 183-bp Cy5-labeled DNA probe,  $P_{hca}$  and 0.05–5.0 nM HcaR protein. 2000 nM unlabeled  $P_{hca}$  was added as a cold probe. **c** DNase I footprint sequencing was performed using purified HcaR protein and a 335-bp DNA probe  $P_{hca}$ . **d** The HcaR binding site in the promoter of *hcaR*. The -10/-35 sequences and the Shine-Dalgarno sequence are underlined and labeled with -10, -35 and SD, respectively. The sequence of the protection region is shown in red. **e** EMSA of the mutant probe Cy5- $P_{hca}(C)$  in the presence of HcaR protein

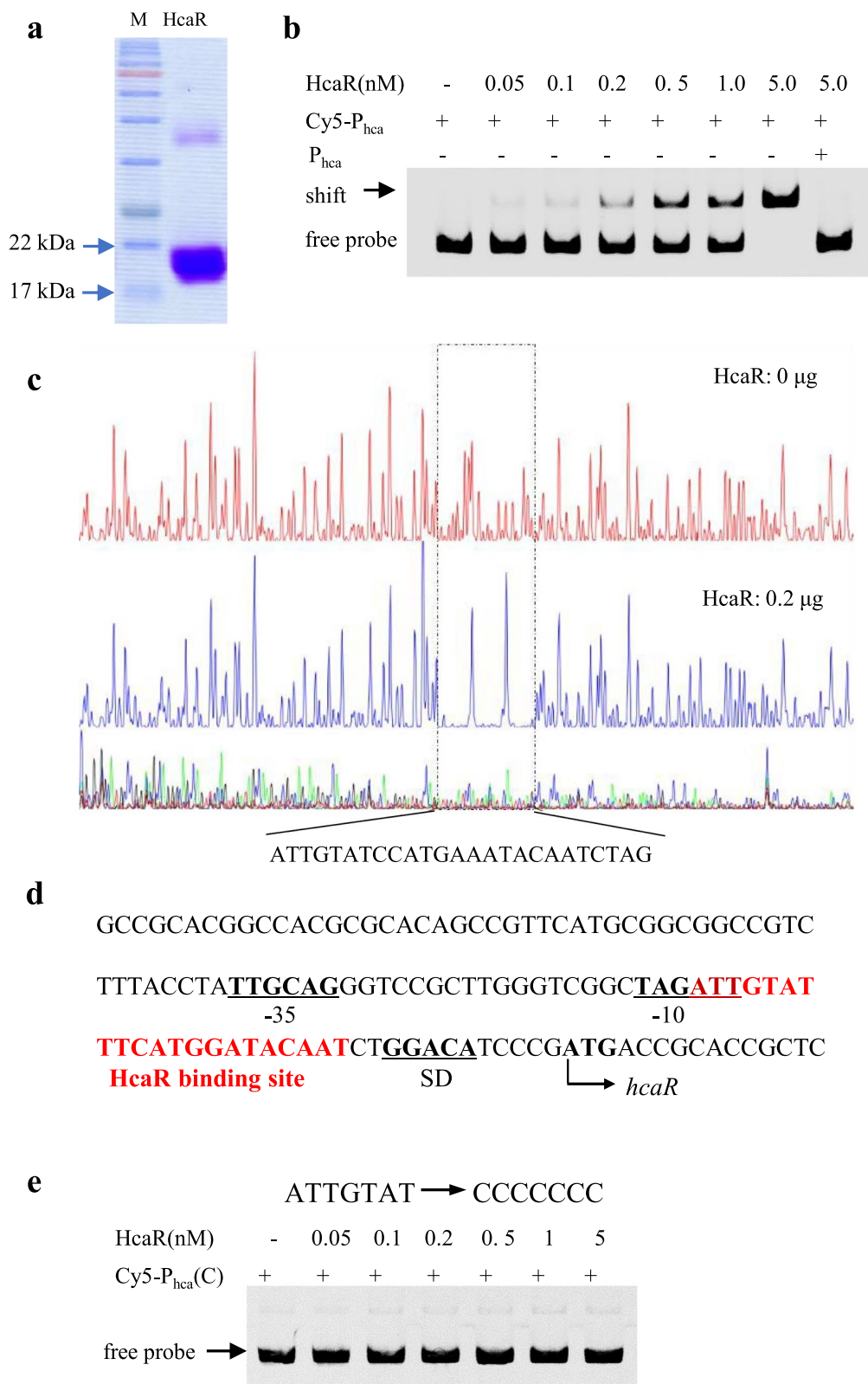


**Fig. 6** (See legend on previous page.)

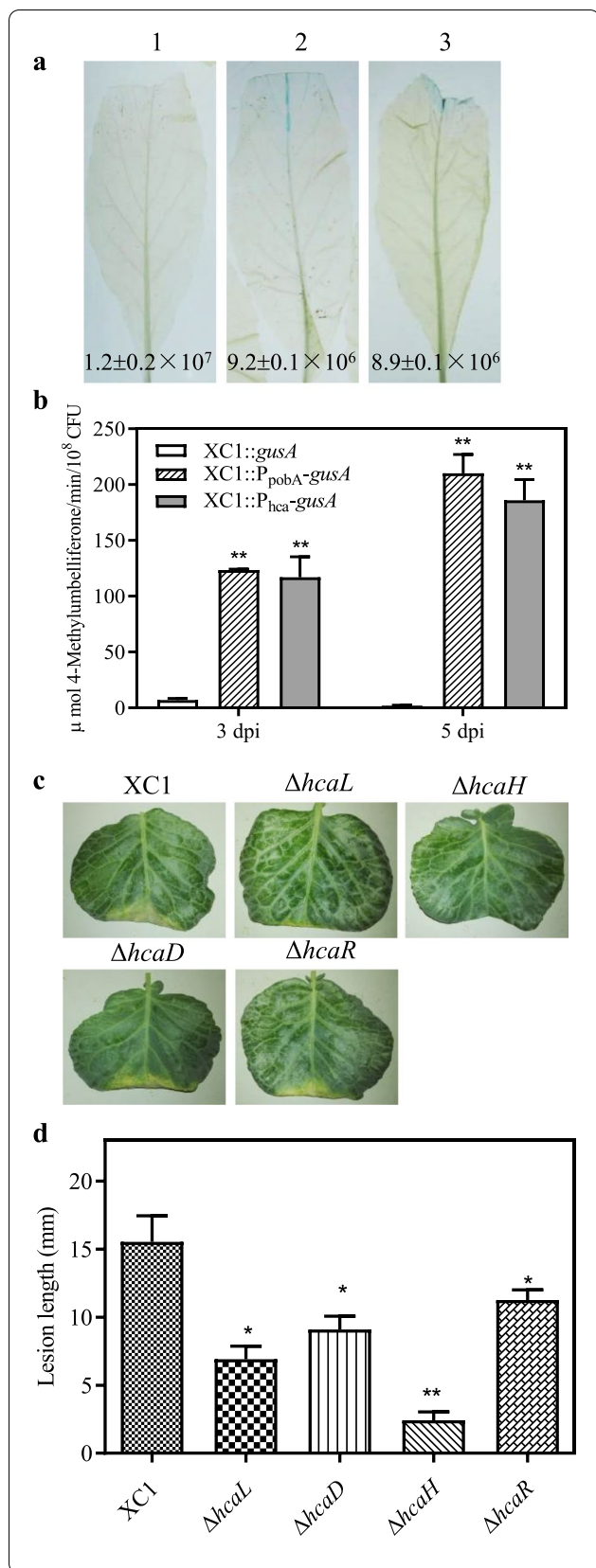


**Fig. 7** Expression of the *hca* promoter in Chinese radish (*Raphanus sativus*) leaves and virulence assays of *hca* gene deletion strains on cabbage (Jingfeng-1) leaves. **a** *Xcc* colony formation units (CFUs) and GUS histochemical staining in infected Chinese radish leaves. 1, XC1::*gusA*; 2, XC1::P<sub>pobA</sub>-*gusA*; 3: XC1::P<sub>hca</sub>-*gusA*. **b** Quantitative analysis of different promoter-driven GUS activities in XC1 strains during infection. **c** Infection lesions by different mutant strains. **d** Quantitative analysis of the infection lesions. The virulence of the *Xcc* strains was tested by measuring lesion length after introducing *Xcc* into the vascular system of cabbage by leaf clipping. Lesion lengths were measured at 15 dpi. Data shown are averages with standard deviations for 15 plants. Values significantly different from that of strain XC1 are indicated by one ( $P < 0.05$ ) or two ( $P < 0.01$ ) asterisks

*X. oryzae* pv. *oryzicola*, *X. oryzae* pv. *oryzae*, *X. fuscans* subsp. *fuscans*, *X. phaseoli* pv. *phaseoli* and *X. albilineans* (Additional file 1: Fig. S8). These findings suggest that HCA degradation is a conserved mechanism in the phytopathogen *Xanthomonas*.

## Discussion

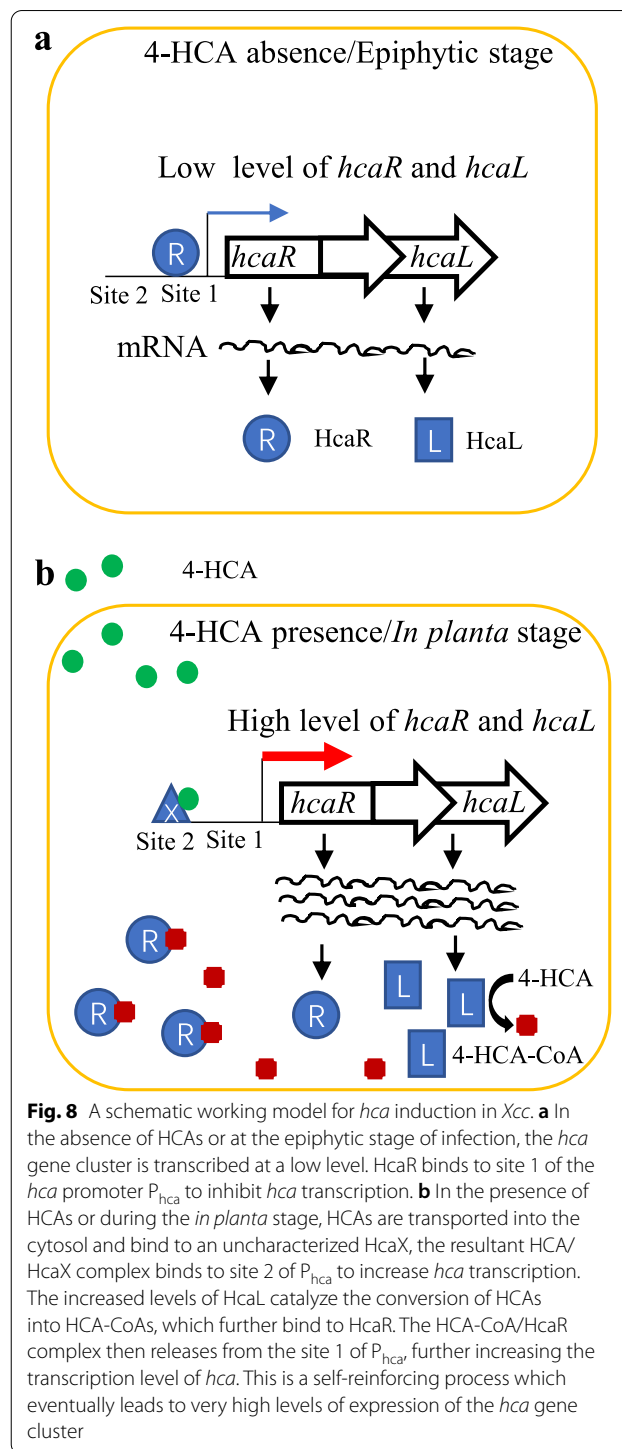
4-HCA, FA, SiA and CA are commonly found in plants; therefore, phytopathogens may experience a complex cocktail of HCAs during infection of their eukaryotic host plants. Using *Xcc* as a model bacterial pathogen, this study for the first time provides a systematic insight into the role of the *hca* gene cluster in HCA degradation and *Xcc* virulence. We also describe a unique HcaR-dependent regulatory mechanism for *hca* transcription. Our results first show that cabbage produces pico-molar levels of 4-HCA, FA, SiA and CA; second, *Xcc* degrades 4-HCA, FA and SiA via the *hca* gene cluster; third, 4-HCA, FA and SiA specifically induce the expression of the *hca* gene cluster for the initiation of the differential degradation of these HCAs; fourth, HCA-derived HCA-CoAs are ligands of HcaR; fifth, HcaR negatively regulates *hca* transcription by binding to a 25-bp region within the promoter P<sub>hca</sub>; sixth, the *hca* gene cluster is expressed by *Xcc* after infection of Chinese radish, at the onset of black rot symptom development; and finally, this gene cluster is required for the full virulence of *Xcc* XC1 on host plants. In light of these findings, it is likely that the degradation of HCAs via the *hca* gene cluster may simultaneously help the pathogen to survive against plant antimicrobial compounds, to spread by reducing physical barriers, and to multiply using HCAs as a carbon source. Given its importance in *Xcc* pathogenicity and its conservation in all *Xanthomonas* species, HCA degradation represents a new type of virulence factor which could be

targeted in the development of new strategies to prevent *Xanthomonas* pathogenesis.

A range of environmental strains and the two phytopathogens *R. solanacearum* and *A. fabrum* were reported to degrade HCA; however, the genes responsible for HCA degradation and the molecular mechanisms for *hca* induction have only been studied in a limited number of strains including *A. fabrum*, *Sphingobium* sp. SYK-6, *Acinetobacter* sp. ADP1, *Pseudomonas fluorescens* BF13 and *R. jostii* RHA1 (Parke and Ornston 2003; Calisti et al. 2008; Kasai et al. 2012; Otani et al. 2016). The precise mechanism of HCA induction of *hca* transcription remains incompletely characterized, although it is widely accepted that the transcription of *hca* genes is induced by HCAs and HcaR is a repressor of *hca* transcription. Consistent with these previous findings, this study showed that the expression of *hca* is specifically induced by 4-HCA, FA and SiA, but not by CA, 4-HBD or vanillin (Fig. 4), and the ligands of HcaR include 4-HCA-CoA, FA-CoA and SiA-CoA (Fig. 5).

In all the previously identified HCA degradation clusters, the regulatory gene encoding HcaR and the degradative enzyme-encoding genes are divergently transcribed, implying a *trans*-regulatory pattern (Otani et al. 2016; Kamimura et al. 2017; Meyer et al. 2018) (Fig. 2a). The present study shows that in all *Xanthomonas* sp, *hcaR* and all other *hca* genes are transcribed within the same operon (Fig. 2a and Additional file 1: Fig. S8). This *cis*-regulatory pattern does not seem sufficient on its own for the regulation of *hca* expression in *Xcc*. Thus, it is possible that an additional, as yet uncharacterized, *trans*-acting regulatory mechanism provides fine tuning of *hca* expression. Based on current knowledge, we propose a schematic working model for *hca* induction in *Xanthomonas* (Fig. 8). In the absence of HCAs or during the epiphytic stage of *Xcc* infection, the *hca* cluster is transcribed at a low level. HcaR binds to site 1 of the *hca* promoter  $P_{hca}$ , allowing a low level of *hca* transcription (Fig. 8a). In the presence of HCAs or during the *in planta* stage, these molecules bind to an uncharacterized sensor protein HcaX and the resultant HCA/HcaX complex binds to site 2 of  $P_{hca}$  to enhance *hca* transcription (Fig. 8b). The increased levels of HcaL catalyzes the conversion of HCAs into HCA-CoAs, which bind to HcaR, and subsequently the HCA-CoA/HcaR complex is released from site 1 of  $P_{hca}$ ; this further increases the transcription of *hca* (Fig. 8b). Future identification of the proposed HcaX could clarify the regulatory mechanism of *hca* transcription.

Lowe et al. (2015) showed that HCA degradation protects *R. solanacearum* from plant chemical defenses and contributes to successful root colonization and virulence. The present study clearly demonstrates the expression



of *hca* during *Xcc* infection of Chinese radish, suggesting that HCA degradation plays a role in *Xcc* pathogenesis. Furthermore, our study also shows that the deletion of individual genes from the *hca* gene cluster significantly reduces *Xcc* virulence in cabbage. Although mutant strains  $\Delta hcaL$ ,  $\Delta hcaH$  and  $\Delta hcaD$  were all significantly

reduced in virulence compared to strain XC1,  $\Delta hcaD$  showed a significantly higher virulence than that of strains  $\Delta hcaL$  and  $\Delta hcaH$  (Fig. 7). This is not surprising since  $\Delta hcaD$  retained considerably higher levels of HCA degradation than those of the other two mutant strains (Fig. 2 and Additional file 1: Fig. S4). In contrast, although strain  $\Delta hcaR$  showed significantly greater degradation of HCAs than strain XC1 as expected, its virulence was significantly lower than that of XC1 (Fig. 7). This inconsistency could be due to the participation of HcaR in other *Xcc* metabolic pathways. Similar findings were also reported in *A. fabrum* C58, in which the MarR family transcriptional regulator HcaR not only negatively regulated HCA degradation, but also modified *virB* gene expression (Meyer et al. 2018). The *A. fabrum hcaR* deletion mutants showed a contrasting competitive colonization ability, being less abundant than the wild-type strain in tumors but more abundant in the rhizosphere (Meyer et al. 2018).

4-HCA, 4-HBA, SiA, vanillic, CA and FA are all found at relatively high concentrations in wastewater effluent from the production of pulp and paper as well as olive oil, and they are also found in waste products from the crop straw utilization industry. The conventional physicochemical methods for degradation of these toxic compounds, include superior processes such as photocatalytic degradation and electrochemical oxidation (Gernjak et al. 2003; Elaoud et al. 2011). Alternatively, microbiological processes for the transformation and degradation of toxic organic pollutants are now promising methods for the remediation of industrial wastewater. Although various bacterial strains are able to metabolize 4-HCA, FA, 4-HBA and CA, few of them are effective with SiA (Xie et al. 2016). With this study, it is now clear that *Xcc* can transform four of these pollutants including SiA with known mechanisms, and the fifth (CA) via an unknown mechanism. Our findings provide a basis for the practical application of *Xanthomonas* in the bioremediation of HCA-contaminated industrial wastewater and soil, and in the synthetic biology for converting HCAs into value-added products.

## Conclusions

*Xcc* efficiently degrades the HCAs 4-HCA, FA and SiA via the *hca* gene cluster. The transcription of *hca* cluster is specifically induced by 4-HCA, FA and SiA, but not by CA. HcaR specifically binds to a 25-bp site within the -10 elements of the *hca* promoter, and negatively regulates *hca* transcription. The *hca* cluster is transcribed *in planta* during pathogenesis of Chinese radish, and *hca* deletion mutant strains exhibit compromised virulence in cabbage. These results suggest that degradation of HCAs contributes to *Xcc* virulence by facilitating its growth and spread.

## Methods

### Bacterial strains and culture conditions

The bacterial strains and plasmids used in the present study are listed in Additional file 2: Tables S1 and S2. In most of our experiments, *Xcc* wild-type strain XC1 and its derivatives were grown at 28 °C in NYG medium (5.0 g/L peptone, 3.0 g/L yeast extract and 20.0 g/L glycerol), whereas *E. coli* strains were grown at 37 °C in LB medium (10 g/L tryptone, 5 g/L yeast extract, 20 g/L NaCl, pH 7.0). Antibiotics were added at the following concentrations when required: rifampicin (Rif) 25 µg/mL, kanamycin (Km) 50 µg/mL, gentamicin (Gm) 20 µg/mL and ampicillin (Amp) 100 µg/mL. Bacterial growth was determined by measuring optical density at a wavelength of 600 nm.

### Gene deletion and functional complementation analysis

*Xcc* in-frame deletion mutants were generated using previously described methods (He et al. 2006); Briefly, the upstream and downstream regions of the target gene (~500 bp) were fused by overlap extension PCR using the primers listed in Additional file 2: Table S3. The fusion product was then subcloned into the suicide vector pK18mobsacB. The resultant recombinant plasmid was introduced into XC1 and integrated into the target DNA via homologous recombination. The resultant strain was then plated on LB agar plate with 50 µg/mL Rif and 5% (w/v) sucrose. PCR and subsequent DNA sequencing were used to verify the deletion mutants. For complementation analysis, the target gene was PCR amplified using the primers listed in Additional file 2: Table S3 and cloned into the multiple cloning site of the expression plasmid pBBR-1-MCS2. The resultant constructs were transferred into *Xcc* by triparental mating.

### Extraction and quantitative analysis of HCA levels in cabbage leaf tissues

Cabbage (Jingfeng-1) was grown in a growth cabinet (NINBO YANGHUI, RND-400B) at 25 °C and 75% humidity with a photoperiod of 16 h (8000 Lx) for two months. HCAs were extracted from 200 mg of leave tissues following previously developed methods (Pan et al. 2010). The dry extracts were then dissolved in 50 µL of methanol, and 5 µL extracts were loaded onto UHPLC-TQT-MS (Agilent, USA) for quantitative analysis, following the procedures described by Chen et al. (2020). Commercially available 4-HCA, FA, SiA and CA (Sigma, USA) were serially diluted to plot standard curves for quantification of endogenous HCA levels in leaf extracts (Additional file 1: Fig. S1).

### Extraction and quantitative analysis of HCAs in *Xcc* cultures by high performance liquid chromatography (HPLC)

HCAs in *Xcc* cultures were extracted and quantified as described previously (Chen et al. 2020). Briefly, 0.5 mL of cell culture was collected at either 12, 24 or 36 hpi, the pH was adjusted to 3.5, and then 1 mL of ethyl acetate was added for the extraction. After evaporation, the dry extract was dissolved in 200  $\mu$ L methanol for HPLC analysis. The HCA levels were quantified using the peak area for the HPLC eluate following the established formula.

### Construction of *gusA*-dependent reporter strains and GUS activity assay

A ~500-bp DNA fragment upstream of the translation initiation codon of the *hca* gene cluster was amplified by PCR using the primer sets in Additional file 2: Table S3. The PCR product was subsequently cloned into the *Bam*HI and *Hind*III sites of the plasmid pMD18T-TOT1-*gusA* (Zhao et al. 2014). DNA fusion fragments harboring the TOT1 terminator, the promoter region and *gusA* gene were amplified by PCR using the primer set TOT1-F and *gusA*-R (Additional file 2: Table S3). The fusion genes were then cloned into the *Sma*I and *Kpn*I sites of pmini-Tn7T-Gm plasmid (Choi and Schweizer 2006) to generate the plasmid mini-P<sub>hca</sub>-*gusA*. The plasmid mini-P<sub>hca</sub>-*gusA* was then integrated into strain XC1 by electroporation as described previously (Choi and Schweizer 2006). GUS activity assays were performed following the protocol described by Chen et al. (2020).

### Protein expression and purification

The *hcaR* coding region was amplified with the primers listed in Additional file 2: Table S3 and fused to the expression vector pET-28a (Merck KgaA, Darmstadt, Germany). The resultant vector was then transformed into the *E. coli* strain BL21(DE3). The expression of HcaR was induced by adding 0.1 mM IPTG to the culture at OD<sub>600</sub> of 0.6 and the culture was subsequently grown at 18 °C for 16 h. Purification of the recombinant protein was by Ni<sup>2+</sup>-affinity chromatography using His-Pur Ni-NTA Resin (Thermo Scientific, Pierce Biotechnology, USA) according to the manufacturer's instructions. HcaR was eluted with buffer containing 20 mM sodium phosphate, 300 mM sodium chloride and 250 mM imidazole (pH 7.4).

### Electrophoretic mobility shift assay (EMSA)

EMSA was performed according to the methods described previously (Chen et al. 2020). The 183-bp DNA probe corresponding to the sequence from -159 to 24 of the *hcaR* promoter region was amplified by PCR using the primer set cy5-P<sub>hca</sub>-F/R. Cy5-labeled probe (10 nM) was incubated with HcaR at a range of concentrations in

EMSA buffer (20 mM Tris pH 7.9, 2 mM DTT, 10 mM MgCl<sub>2</sub>, 5% glycerol, 40  $\mu$ g/mL BSA, 100 ng/mL sonicated salmon sperm DNA). To verify the specificity of the binding, 2000 nM unlabeled probe was amplified and added as a specific competitor. After incubation at 25 °C for 30 min, the reaction mixture was electrophoresed at 4 °C on a 4.5% native polyacrylamide gel in 0.5  $\times$  Tris-borate-EDTA (TBE) buffer for 45 min at 125 V. The gels were scanned for fluorescent DNA using the Starion FLA-9000 Scanner (FujiFilm, Japan).

### DNase I footprinting sequencing assay

The fluorescent FAM-labeled probes were amplified by PCR with Dpx DNA polymerase using the primer set of M13F-47 (FAM) and M13R-48 and plasmid pUC19-T-P<sub>hca</sub> as a template. DNase I footprinting assays were conducted in TOLO Biotech, Shanghai following a protocol described previously (Wang et al. 2012).

### Plant GUS histochemical staining assay and bacterial CFU determination *in planta*

*Xcc* strains were cultured in NYG liquid medium overnight, adjusted to an OD<sub>600</sub> of 0.1 (1.0  $\times$  10<sup>8</sup> CFU/mL), and were then used to inoculate the leaves of Chinese radish (*Raphanus sativus* Manshenhong) using the leaf clipping method (Li et al. 2014). At 3 and 5 dpi, the infected leaves were collected for GUS histochemical staining and  $\beta$ -glucuronidase activity analysis following the procedure by Li et al. (2014). *Xcc* CFU *in planta* were also quantified in a parallel experiment. For each strain, three leaves were chosen for GUS staining and 5 leaves for CFU quantification in each experiment; the experiments were repeated twice. *Xcc* strains harboring the plasmids pLAFR3 or pGUShrpX (Li et al. 2014) were used as negative and positive controls, respectively.

### Virulence assay in cabbage

The virulence of *Xcc* in cabbage (*Brassica oleracea*) cultivar Jingfeng-1 was tested by the leaf-clipping method (Chen et al. 2020). The third true leaf of 2-month-old cabbage plants were inoculated with sterile scissors dipped in bacterial suspensions (OD<sub>600</sub> value of 0.1). Lesion length was measured at 15 dpi. For each strain, a total of 15 plants were inoculated and the average lesion lengths with standard deviation are shown.

### Statistical analysis

All experiments were performed at least three times unless otherwise stated. ANOVA for experimental data sets was performed using JMP software version 5.0 (SAS Institute Inc., Cary, NC). Significant effects of treatment were determined by the F value ( $P=0.05$ ). When a

significant F test was obtained, separation of means was accomplished by Fisher's protected LSD (least significant difference) test at  $P < 0.05$ .

### Abbreviations

2-HCA: 2-Hydroxycinnamic acid; 3-HCA: 3-Hydroxycinnamic acid; 4-HBA: 4-Hydroxybenzoic acid; 4-HCA: 4-Hydroxycinnamic acid; 4-HCA-CoA: 4-Hydroxycinnamoyl-CoA; CA: Caffeic acid; CoA: Coenzyme A; FA: Ferulic acid; FA-CoA: Feruloyl CoA; HCAs: Hydroxycinnamic acids; HMMPHP-CoA: (3,5-Dimethoxy-4-hydroxyphenyl)-propionyl-CoA; HMPHP-CoA: (3-Methoxy-4-hydroxyphenyl)-propionyl-CoA; HTH: Helix-turn-helix; NYG medium: Peptone yeast glycerol medium; PCA: Protocatechuate; RT-PCR: Reverse transcription-PCR; SiA: Sinapic acid; SiA-CoA: Sinapoyl CoA; T3SS: Type III secretion system; TBE: Tris-borate-EDTA; UHPLC-TQT-MS: Ultra-High Performance Liquid Chromatography coupled with Triple Quadrupole Tandem Mass Spectrometry; *Xcc*: *X. campestris* P.v. *campestris*.

### Supplementary Information

The online version contains supplementary material available at <https://doi.org/10.1186/s42483-022-00119-z>.

**Additional file 1. Fig. S1.** HPLC-Triple Quadrupole Mass Spectrometry analysis of 4-HCA and FA. **a** Parameters used for HPLC-Triple Quadrupole Mass analysis of 4-HCA and FA. **b** The mass spectrometry spectrum of 4-HCA and FA. **c, d** The plotted standard curve between peak area and the concentration of 4-HCA and FA. **Fig. S2.** CA degradation in strain XC1 and several *hca* gene cluster mutant strains. **a** Time course of HCA levels in NYG medium. **b** Growth time course of XC1 and mutant strains in NYG medium supplemented with 50  $\mu$ M CA. **c** Time course of CA degradation in XC1 and XC1-derived strains grown in NYG medium supplemented with 50  $\mu$ M CA. Three independent experiments were conducted and data are shown as averages with standard deviations. **Fig. S3.** Genomic analysis of the *hca* gene cluster in *Xcc* strains. **a** The *hca* gene cluster in *Xcc* strains b100, ATCC33913 and 8004. **b** The *hcaD* DNA sequence in ATCC33913 and 8004. **c** *hcaD* in *Xcc* strain XC1. **Fig. S4.** FA and SiA degradation by the *hca* gene cluster. **a, c** Growth time course of XC1 and XC1-derived strains in NYG medium supplemented with 50  $\mu$ M FA or SiA. **b, d** Time course of FA and SiA degradation by XC1 and XC1-derived strains in NYG liquid culture supplemented with 50  $\mu$ M FA or SiA. **e** The proposed FA and SiA degradation pathways in *Xcc*. HMPHP-CoA, (3-methoxy-4-hydroxyphenyl)-propionyl-CoA; PCA, protocatechuate; HMMPHP-CoA, (3, 5-dimethoxy-4-hydroxyphenyl)-propionyl-CoA. For **a–d**, three independent experiments were conducted for each and the averages with standard deviations are shown. **Fig. S5.** Construction of *gusA* transcriptional reporter strains. **a** The cloned putative promoter regions for detection of transcriptional activity. **b** Schematic representation of the promoter-*gusA* reporter strain. **Fig. S6.** The evidence for HcaR dimer formation. **a** The standard relationship between protein size and elution volume on a Superdex 200 column in Tris buffer (10 mM Tris, 150 mM NaCl, 5% glycerol, pH 7.5). **b, c** Size exclusion chromatography analysis of HcaR in Tris buffer. **Fig. S7.** Conservation analysis of the HcaR binding site in *Xanthomonas* strains. **Xcc**: *X. campestris* pv. *campestris* XC1; **Xoc**: *X. oryzae* pv. *oryzicola* BLS256; **Xcci**: *X. citri* pv. *citri* 306; **Xpp**: *X. phaseoli* pv. *phaseoli* CFBP6164; **Xff**: *X. fuscans* subsp. *fuscans* 4834R; **Xcv**: *X. campestris* pv. *vesicatoria* 85–10; **Xci**: *X. citri* subsp. *citri* Aw12879; **Xoo**: *X. oryzae* pv. *oryzae* PXO99A; **Xcr**: *X. campestris* pv. *raphani* 756C. **Fig. S8.** Conservation analysis of the 4-HCA gene cluster in *Xanthomonas* strains. **Xcc**: *X. campestris* pv. *campestris* XC1; **Xac**: *X. citri* pv. *citri* 306; **Xcr**: *X. campestris* pv. *raphani* 756C; **Xcv**: *X. campestris* pv. *vesicatoria* 85–10; **Xcci**: *X. citri* subsp. *citri* Aw12879; **Xoc**: *X. oryzae* pv. *oryzicola* BLS256; **Xoo**: *X. oryzae* pv. *oryzae* PXO99A; **Xff**: *X. fuscans* subsp. *fuscans* 4834R; **Xpp**: *X. phaseoli* pv. *phaseoli* CFBP6164; **Xa**: *X. albilineans* GPE PC73.

**Additional file 2. Table S1.** Bacterial strains used in this study. **Table S2.** Plasmids used in this study. **Table S3.** Oligonucleotide primers used in this study.

### Acknowledgements

We thank Prof. Guang-Tao Lu at Guangxi University for discussions and technical help with GUS staining.

### Author contributions

YWH conceived the experimental design, interpreted the results and wrote the manuscript. ARP and LZ participated in the interpretation of the results and writing of the manuscript. BC, RFL and LZ performed the experiments. KS developed the assay method for promoter analysis. All authors read and approved the final manuscript.

### Funding

This work was financially supported by research grants from the National Natural Science Foundation of China (No. 31972231 to HYW, No. 32172355 to HYW).

### Availability of data and materials

Not applicable.

### Declarations

### Ethics approval and consent to participate

Not applicable.

### Consent for publication

Not applicable.

### Competing interests

The authors declare that they have no competing interests.

### Author details

<sup>1</sup>State Key Laboratory of Microbial Metabolism, Joint International Research Laboratory of Metabolic and Developmental Sciences, School of Life Sciences and Biotechnology, Shanghai Jiao Tong University, Shanghai 200240, China. <sup>2</sup>Guangxi Key Laboratory of Biology for Crop Diseases and Insect Pests, Plant Protection Research Institute, Guangxi Academy of Agricultural Sciences, Nanning 530007, Guangxi, China. <sup>3</sup>Zhiyuan Innovative Research Centre, Student Innovation Institute, Zhiyuan College, Shanghai Jiao Tong University, Shanghai, China. <sup>4</sup>Department of Entomology, Plant Pathology and Nematology, University of Idaho, Moscow, ID 83844, USA.

Received: 21 February 2022 Accepted: 1 April 2022

Published online: 20 April 2022

### References

- Bertani I, Kojic M, Venturi V. Regulation of the *p*-hydroxybenzoic acid hydroxylase gene (*pobA*) in plant-growth-promoting *Pseudomonas putida* WCS358. *Microbiology*. 2001;147(6):1611–20. <https://doi.org/10.1099/00221287-147-6-1611>.
- Calero P, Jensen SI, Bojanović K, Lennen RM, Koza A, Nielsen AT. Genome-wide identification of tolerance mechanisms toward *p*-coumaric acid in *Pseudomonas putida*. *Biotechnol Bioeng*. 2018;115(3):762–74. <https://doi.org/10.1002/bit.26495>.
- Calisti C, Ficca AG, Barghini P, Ruzzi M. Regulation of ferulic catabolic genes in *Pseudomonas fluorescens* BF13: involvement of a MarR family regulator. *Appl Microbiol Biotechnol*. 2008;80:475–83. <https://doi.org/10.1007/s00253-008-1557-4>.
- Campillo T, Renoud S, Kerzaon I, Vial L, Baude J, Gaillard V, et al. Analysis of hydroxycinnamic acid degradation in *Agrobacterium fabrum* reveals a coenzyme A-dependent, beta-oxidative deacetylation pathway. *Appl Environ Microbiol*. 2014;80(11):3341–9. <https://doi.org/10.1128/AEM.00475-14>.
- Campos L, Lisón P, López-Gresa MP, Rodrigo I, Zacarés L, Conejero V, et al. Transgenic tomato plants overexpressing tyramine N-hydroxycinnamoyl-transferase exhibit elevated hydroxycinnamic acid amide levels and enhanced resistance to *Pseudomonas syringae*. *Mol Plant Microbe Interact*. 2014;27(10):1159–69. <https://doi.org/10.1094/MPMI-04-14-0104-R>.

- Cao XQ, Ouyang XY, Chen B, Song K, Zhou L, Jiang BL, et al. Genetic interference analysis reveals that both 3-hydroxybenzoic acid and 4-hydroxybenzoic acid are involved in xanthomonadin biosynthesis in the phytopathogen *Xanthomonas campestris* pv. *campestris*. *Phytopathology*. 2020;110(2):278–86. <https://doi.org/10.1094/PHYTO-08-19-0299-R>.
- Cartea ME, Francisco M, Soengas P, Velasco P. Phenolic compounds in *Brassica* vegetables. *Molecules*. 2010;16(1):251–80. <https://doi.org/10.3390/molecules16010251>.
- Chen B, Li RF, Zhou L, Qiu JH, Song K, Tang JL, et al. The phytopathogen *Xanthomonas campestris* utilizes the divergently transcribed *pobA/pobR* locus for 4-hydroxybenzoic acid recognition and degradation to promote virulence. *Mol Microbiol*. 2020;114(5):870–86. <https://doi.org/10.1111/mmi.14585>.
- Choi KH, Schweizer HP. Mini-Tn7 insertion in bacteria with single attTn7 sites: example *Pseudomonas aeruginosa*. *Nat Protoc*. 2006;1(1):153–61. <https://doi.org/10.1038/nprot.2006.24>.
- Elaoud SC, Panizza M, Cerisola G, Mgru T. Electrochemical degradation of sinipinic acid on a BDD anode. *Desalination*. 2011;272(1–3):148–53. <https://doi.org/10.1016/j.desal.2011.01.011>.
- El-Seedi HR, El-Said AM, Khalifa SA, Göransson U, Bohlin L, Borg-Karlson AK, et al. Biosynthesis, natural sources, dietary intake, pharmacokinetic properties, and biological activities of hydroxycinnamic acids. *J Agric Food Chem*. 2012;60(44):10877–95. <https://doi.org/10.1021/jf301807g>.
- Fan S, Tian F, Li J, Hutchins W, Chen H, Yang F, et al. Identification of phenolic compounds that suppress the virulence of *Xanthomonas oryzae* on rice via the type III secretion system. *Mol Plant Pathol*. 2017;18(4):555–68. <https://doi.org/10.1111/mpp.12415>.
- Fuchs G, Boll M, Heider J. Microbial degradation of aromatic compounds—from one strategy to four. *Nat Rev Microbiol*. 2011;9(11):803–16. <https://doi.org/10.1038/nrmicro2652>.
- Gernjak W, Krutzler T, Glaser A, Malato S, Caceres J, Bauer R, et al. Photo-Fenton treatment of water containing natural phenolic pollutants. *Chemosphere*. 2003;50(1):71–8. [https://doi.org/10.1016/s0045-6535\(02\)00403-4](https://doi.org/10.1016/s0045-6535(02)00403-4).
- Harris V, Jiranek V, Ford CM, Grbin PR. Inhibitory effect of hydroxycinnamic acids on *Dekkera* spp. *Appl Microbiol Biotechnol*. 2010;86(2):721–9. <https://doi.org/10.1007/s00253-009-2352-6>.
- He YW, Xu M, Lin K, Ng YJA, Wen CM, Wang LH, et al. Genome scale analysis of diffusible signal factor regulon in *Xanthomonas campestris* pv. *campestris*: identification of novel cell-cell communication-dependent genes and functions. *Mol Microbiol*. 2006;59(2):160–22. <https://doi.org/10.1111/j.1365-2958.2005.04961.x>.
- Hirakawa H, Schaefer AL, Greenberg EP, Harwood CS. Anaerobic *p*-coumarate degradation by *Rhodospseudomonas palustris* and identification of CouR, a MarR repressor protein that binds *p*-coumaroyl coenzyme A. *J Bacteriol*. 2012;194(8):1960–7. <https://doi.org/10.1128/JB.06817-11>.
- Kamimura N, Takahashi K, Mori K, Araki T, Fujita M, Higuchi Y, et al. Bacterial catabolism of lignin-derived aromatics: New findings in a recent decade: update on bacterial lignin catabolism. *Environ Microbiol Rep*. 2017;9(6):679–705. <https://doi.org/10.1111/1758-2229.12597>.
- Kasai D, Kamimura N, Tani K, Umeda S, Abe T, Fukuda M, et al. Characterization of FerC, a MarR-type transcriptional regulator, involved in transcriptional regulation of the ferulate catabolic operon in *Sphingobium* sp. strain SYK-6. *FEMS Microbiol Lett*. 2012;332(1):68–75. <https://doi.org/10.1111/j.1574-6968.2012.02576.x>.
- Lanoue A, Burlat V, Henkes GJ, Koch I, Schurr U, Röse US. *De novo* biosynthesis of defense root exudates in response to *Fusarium* attack in barley. *New Phytol*. 2010;185(2):577–88. <https://doi.org/10.1111/j.1469-8137.2009.03066.x>.
- Li Y, Peng Q, Selimi D, Wang Q, Charkowski AO, Chen X, et al. The plant phenolic compound *p*-coumaric acid represses gene expression in the *Dickeya dadantii* type III secretion system. *Appl Environ Microbiol*. 2009;75(5):1223–8. <https://doi.org/10.1128/AEM.02015-08>.
- Li RF, Lu GT, Li L, Su HZ, Feng GF, Chen Y, et al. Identification of a putative cognate sensor kinase for the two-component response regulator HrpG, a key regulator controlling the expression of the *hrp* genes in *Xanthomonas campestris* pv. *campestris*. *Environ Microbiol*. 2014;16(7):2053–71. <https://doi.org/10.1111/1462-2920.12207>.
- Lin LZ, Harnly JM. Phenolic component profiles of mustard greens, yu choy, and 15 other *Brassica* vegetables. *J Agric Food Chem*. 2010;58(11):6850–7. <https://doi.org/10.1021/jf1004786>.
- Liu QQ, Luo L, Zheng LQ. Lignins: biosynthesis and biological functions in plants. *Int J Mol Sci*. 2018;19(2):335. <https://doi.org/10.3390/ijms19020335>.
- Lowe TM, Ailloud F, Allen C. Hydroxycinnamic acid degradation, a broadly conserved trait, protects *Ralstonia solanacearum* from chemical plant defenses and contributes to root colonization and virulence. *Mol Plant Microbe Interact*. 2015;28(3):286–97. <https://doi.org/10.1094/MPMI-09-14-0292-FI>.
- Mansfield J, Genin S, Magori S, Citovsky V, Sriariyanum M, Ronald P, et al. Top 10 plant pathogenic bacteria in molecular plant pathology. *Mol Plant Pathol*. 2012;13(6):614–29. <https://doi.org/10.1111/j.1364-3703.2012.00804.x>.
- Meyer T, Renoud S, Vigouroux A, Miomandre A, Gaillard V, Kerzoon I, et al. Regulation of hydroxycinnamic acid degradation drives *Agrobacterium fabrum* life styles. *Mol Plant Microbe Interact*. 2018;31(8):814–22. <https://doi.org/10.1094/MPMI-10-17-0236-R>.
- Naoumkina MA, Zhao Q, Gallego-Giraldo L, Dai X, Zhao PX, Dixon RA. Genome-wide analysis of phenylpropanoid defence pathways. *Mol Plant Pathol*. 2010;11(6):829–46. <https://doi.org/10.1111/j.1364-3703.2010.00648.x>.
- Olsen H, Aaby K, Borge GI. Characterization and quantification of flavonoids and hydroxycinnamic acids in curly kale (*Brassica oleracea* L. convar. *acephala* var. *sabellica*) by HPLC-DAD-ESI-MSn. *J Agric Food Chem*. 2009;57(7):2816–25. <https://doi.org/10.1021/jf803693t>.
- Otani H, Stogios PJ, Xu X, Nocek B, Li SN, Savchenko A, et al. The activity of CouR, a MarR family transcriptional regulator, is modulated through a novel molecular mechanism. *Nucleic Acids Res*. 2016;44(2):595–607. <https://doi.org/10.1093/nar/gkv955>.
- Pan X, Welti R, Wang X. Quantitative analysis of major plant hormones in crude plant extracts by high-performance liquid chromatography-mass spectrometry. *Nat Protoc*. 2010;5(6):986–92. <https://doi.org/10.1038/nprot.2010.37>.
- Parke D, Ornston LN. Hydroxycinnamate (*hca*) catabolic genes from *Acinetobacter* sp. strain ADP1 are repressed by HcaR and are induced by hydroxycinnamoyl-coenzyme A thioesters. *Appl Environ Microbiol*. 2003;69(9):5398–409. <https://doi.org/10.1128/AEM.69.9.5398-5409.2003>.
- Plaggenborg R, Overhage J, Steinbüchel A, Priefert H. Functional analyses of genes involved in the metabolism of ferulic acid in *Pseudomonas putida* KT2440. *Appl Microbiol Biotechnol*. 2003;61(5–6):528–35. <https://doi.org/10.1007/s00253-003-1260-4>.
- Timilsina S, Potnis N, Newberry EA, Liyanapathirana P, Iruegas-Bocardo F, White FF, et al. *Xanthomonas* diversity, virulence and plant-pathogen interactions. *Nat Rev Microbiol*. 2020;18(8):415–27. <https://doi.org/10.1038/s41579-020-0361-8>.
- Vicente JG, Holub EB. *Xanthomonas campestris* pv. *campestris* (cause of black rot of crucifers) in the genomic era is still a worldwide threat to brassica crops. *Mol Plant Pathol*. 2013;14(1):2–18. <https://doi.org/10.1111/j.1364-3703.2012.00833.x>.
- Wallis CM, Chen J. Grapevine phenolic compounds in xylem sap and tissues are significantly altered during infection by *Xylella fastidiosa*. *Phytopathology*. 2012;102(9):816–26. <https://doi.org/10.1094/PHYTO-04-12-0074-R>.
- Wang Y, Cen XF, Zhao GP, Wang J. Characterization of a new GlnR binding box in the promoter of *amtB* in *Streptomyces coelicolor* inferred the PhoP/GlnR competitive binding mechanism for transcriptional regulation of *amtB*. *J Bacteriol*. 2012;194(19):5237–44. <https://doi.org/10.1128/JB.00989-12>.
- Wang JY, Zhou L, Chen B, Sun S, Zhang W, Li M, et al. A functional 4-hydroxybenzoate degradation pathway in the phytopathogen *Xanthomonas campestris* is required for full pathogenicity. *Sci Rep*. 2015;5:18456. <https://doi.org/10.1038/srep18456>.
- Xie XG, Huang CY, Fu WQ, Dai CC. Potential of endophytic fungus *Phomopsis liquidambari* for transformation and degradation of recalcitrant pollutant sinapic acid. *Fungal Biol*. 2016;120(3):402–13. <https://doi.org/10.1016/j.funbio.2015.11.010>.
- Yang S, Peng Q, San Francisco M, Wang Y, Zeng Q, Yang CH. Type III secretion system genes of *Dickeya dadantii* 3937 are induced by plant phenolic acids. *PLoS ONE*. 2008;3(8): e2973. <https://doi.org/10.1371/journal.pone.0002973>.
- Zhao ZH, Xiong L, Shen CW, Sun QB, Zou LF, Chen GY. Construction of two promoter-probe vectors suitable for pathogenicity-related gene expression analysis in *Xanthomonas oryzae* pv. *oryzicola*. *Acta Phytopathol Sin*. 2014;44(5):504–511. <https://doi.org/10.13926/j.cnki.apps.2014.05.008>.
- Zhou L, Wang JY, Wu J, Poplawsky A, Lin SJ, Zhu BS, et al. The diffusible factor synthase XanB2 is a bifunctional chorismatase that links the shikimate pathway to ubiquinone and xanthomonadine biosynthetic pathways. *Mol Microbiol*. 2013;87(1):80–93. <https://doi.org/10.1111/mmi.12084>.

## Publisher's Note

Springer Nature remains neutral with regard to jurisdictional claims in published maps and institutional affiliations.